SACLANTCEN REPORT
serial no: SR- 329

SACLANT UNDERSEA RESEARCH CENTRE REPORT

NORTH ATLANTIC TREATY ORGANIZATION ORGANISATION DU TRAITE DE L'ATLANTIQUE NORD

Aspects of Cardioid Processing.

D.T. Hughes

The content of this document pertains to work performed under Project 04-A of the SACLANTCEN Programme of Work. The document has been approved for release by The Director, SACLANTCEN.

Jan L. Spoelstra
Director

intentionally blank page

Aspects of Cardioid Processing.

D.T. Hughes

Executive Summary: Traditional active towed array sonar systems suffer from the problem of ambiguous returns: in which a sonar operator cannot ascertain whether a possible target is placed to the port or to starboard. Although operational methods exist for overcoming this problem they are time-consuming and cannot usually be used for a single ping.

Several NATO nations are investigating 'triplet technology' to allow port-starboard (left-right) discrimination. SACLANT Undersea Research Centre has purchased a broad-band triplet array to investigate the use and implementation of this important and relevant technology.

This report describes, in detail, two modes of operation of the triplet array. These methods are investigated for SNR performance and compared for correlated and uncorrelated noise. The latter is expected to play a crucial role in this technology for which intra-triplet hydrophones are closely spaced. Both methods are shown to give excellent results on real data, with a typical Left-Right suppression of greater than 15dB, allowing unambiguous determination of target bearing as well as reverberation suppression.

intentionally blank page

Aspects of Cardioid Processing.

D.T. Hughes

Abstract:

It is well known that conventional active towed arrays suffer from 'The Ambiguity Problem' in which it is impossible to distinguish returns from port or starboard. Although operational methods for overcoming this problem exist they are time-consuming and cannot be used for a single ping. One proposed method of coping with these difficulties is to use a triplet array in which the direction of arrival of a signal can be ascertained on a single ping.

This report details a broadband algorithm which has been developed and is currently being used at the Saclant Undersea Research Centre. The algorithm was specifically designed to be used on a delay-type beamformer in which shading cannot be applied at the beamlevel. A second algorithm employing the full-flexability of a 3d beamformer is also described and the two algorithms are compared for their performance in terms of left-right suppression and SNR for which analytical expressions are computed. It is shown that both of the algorithms have desirable but different features. The algorithms are applied to data taken from the trial BACCHUS'98 and the results obtained are used to help validate the theoretical results and to give an indication of the performance which is achievable for the triplet system. We show that for the Centre algorithm a typical achievable left-right suppression is greater than 15dB.

Keywords:

Cardioid Processing, left-right suppression, towed array sonar,

Contents

1

Introduction

Several NATO nations have an active research and development program investigating aspects of Left-Right suppression/discrimination (including UK, France, The Netherlands and Germany). [1, 2, 3]

The present operational means of discriminating whether a particular sonar return is from port or starboard, in effect necessitates, tracking a contact over many pings from a manoeuvering platform. The techniques which are currently under investigation, however, discriminate on a single ping.

Various means exist for carrying out this discrimination including:

i) directional transmitters; in which different pulses are transmitted to port and starboard.

ii) Twin (or multiple) arrays; in which two or more line arrays are towed parallel with, in the twin case, a spacing of approximately quarter of a wavelength of the highest frequency.

iii) Cardioid technology. This can be further broken into two areas of interest. It is possible to produce directional transducers allowing an array to be made which is actually formed from a left and a right looking array 'hard-wired in'. The alternative approach is to produce an array made up of triplets of sensors with all channels digitized and sent back to a central processor so that beamforming and hydrophone sensitivity can be controlled in real time.

It is this last technique which we shall investigate in this report. Figure 1 shows an artists impression of such an array. Each triplet (for example that marked ABC on the figure) provides 3 channels of acoustic data. The individual triplets may be rotated away from the vertical but the degree of rotation will be known fairly accurately due to roll sensors positioned along the array. (We discuss in annex E the effect of errors in this measurement). Generally the array is constructed in such a way as to stop the array from rotating too severely whilst being towed.

SACLANT Research Centre obtained a broadband cardioid array in 1999. This report details the proposed algorithm for use in the Centre's system. It goes on to discuss alternative algorithms, and details certain important operational features of

a cardioid array.

The philosophy of this report is to give the main algorithm and indication of results in the body of the text whilst leaving the detailed mathematical investigation to the annexes.

In section 2 we detail the algorithm which is to be used in the Centre's array. This algorithm needs to be broadband and implementable on a delay beamformer. We refer to this algorithm here and throughout the report as the 'Centre-algorithm'. The general approach is to do the beamforming in two phases. The first is done at the triplet level using signal processing to form a cardioid responses before doing the processing in the azimuthal plane.

In sections 3 and 4 we briefly discuss the philosophy and operating parameters of the BACCHUS'98 trial as well as giving some typical results using the algorithm of section 2. In section 5 we draw conclusions and make recommendations based on the main body of the text and from the annexes.

In annex A we show how the algorithm of section 2 can be obtained as an approximation of an optimum (in a least mean squares sense) beamformer with the constraint of real weights.

In annex B we discuss one possible alternative algorithm which may be employed on a triplet array. We refer to this as the '3d-algorithm' since it treats the array as a whole rather than breaking it into the individual triplets as for the Centre-algorithm.

In annexes C and D we compare the Centre-algorithm and the 3d-algorithm in terms of SNR and left-right suppression statistics.

In annex E we briefly consider how the algorithms are affected by system errors and approximations.

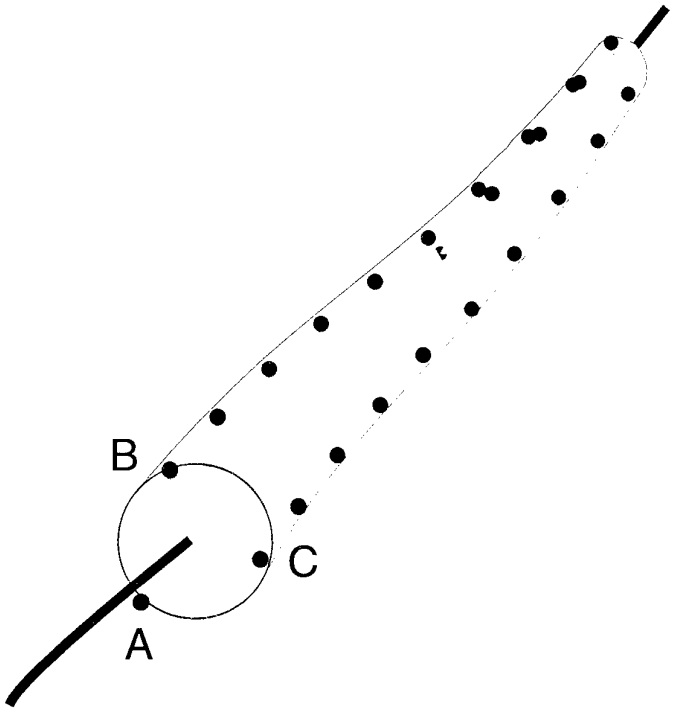

Figure 1 *Artist's impression of Cardioid Array. The triangle ABC represents a triplet of the array which provides three channels of acoustic data.*

2

Broadband Cardioid Processing

The array obtained by SACLANT Undersea Research Centre, as well as being directional has been designed to be used for broadband research, with a bandwidth of approximately 2.5kHz. Consequently any proposed algorithm must be amenable to broadband processing. Also the algorithm should be implementable in a time-domain delay, beamformer rather than in the frequency domain. Furthermore, due to the nature of the Centre's real-time system, when this research was being carried out, shading cannot be applied at the beam level. Subsequent upgrades to the system have removed this restriction but the algorithm detailed here will be continued to be used in the forseeable future. Such problems have recently received some theoretical consideration in the literature [5]. In annex B we discuss another algorithm which although in someways is superior to the Centre algorithm requires a frequency domain implementation.

It is also worth mentioning at this point that other algorithms can be envisaged and the exact form that we expect an algorithm to take is dependent on what is desired from the final system. For instance in the two algorithms investigated in this report we do not use the 'vertical' extension of the triplet which would allow, for instance, a null to be driven towards the surface to allow suppression of surface noise. Such research although interesting and worthwhile is beyond the scope of this report.

In what follows we assume that there are N_c triplets ($3N_c$ hydrophones). The hydrophones are numbered

$$\begin{aligned}
&(\overbrace{x_{11}, x_{21}, x_{31}}^{\text{first triplet}}, \ldots\ldots\ldots \overbrace{x_{1N}, x_{2N}, x_{3N}}^{\text{last triplet}}) \\
&(y_{11}, y_{21}, y_{31}, \ldots\ldots\ldots y_{1N}, y_{2N}, y_{3N}) \\
&(z_{11}, z_{21}, z_{31}, \ldots\ldots\ldots z_{1N}, z_{2N}, z_{3N}).
\end{aligned} \tag{1}$$

Figure 2 shows the co-ordinate system used in the following exposition. ABC is one triplet of hydrophones lying on an equilateral triangle, the plane of which is perpendicular to the tow direction $\phi = 0$. We shall ignore the θ dependence, only considering the horizontal plane for which $\theta = \frac{\pi}{2}$. The desired beam is, then, steered towards $(\theta = \frac{\pi}{2}, \phi = \phi_0)$.

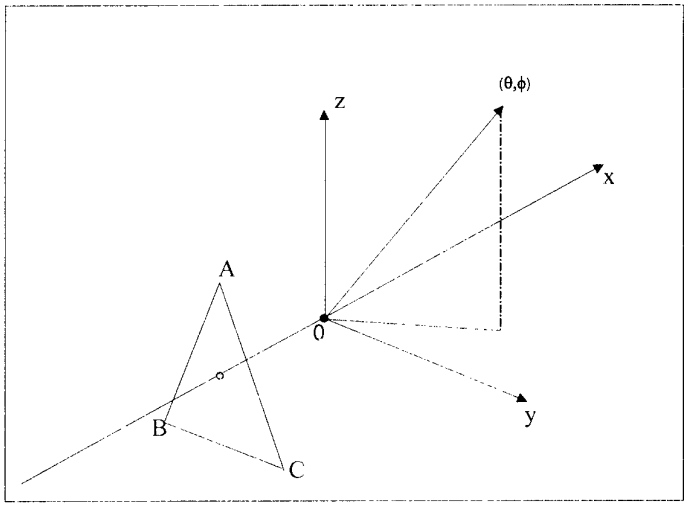

Figure 2 *Co-ordinate system used in the report. The azimuthal, horizontal plane has* $\theta = \frac{\pi}{2}$. *The x-axis is defined by the direction* $(\theta = \frac{\pi}{2}, \phi = 0)$.

The response of the beamformer, to a plane wave coming from the direction ϕ at one frequency f, is

$$r(\phi, f) = \sum_{j=1}^{N} \exp(-2\pi i f \tau^j) \sum_{k=1}^{3} \alpha_c^{kj} \exp(\frac{2\pi}{c} f i (x_{kj} \cos\phi + y_{kj} \sin\phi - c\tau_c^{kj}) \qquad (2)$$

c is the speed of sound, the τ's and τ_c's are delays the latter representing delays associated with the individual triplets and the α_cs are the individual hydrophone weightings ordered on the triplets.

If we note that, for an idealised, non-snaking, array, $x_{kj} \equiv x_j$ since the x co-ordinates are constant within a particular triplet:

$$r(\phi, f) = \sum_{j=1}^{N} \exp(\frac{-2\pi i f}{c}(x_j cos\phi - c\tau^j)) \sum_{k=1}^{3} \alpha_c^{kj} \exp(\frac{2\pi}{c} f i (y_{kj} \sin\phi - c\tau_c^{kj})) \qquad (3)$$

α_c^{kj} is necessarily chosen real (because of the constraints of Saclant Centre's present real time system).

It was found after some investigation (see annex A for proof and annex E for limitations) that cardioid beampatterns are formed in individual triplets if $\alpha_c^{kj} = \sin \mu_c^i$ where μ_c^i is the angular displacement of the triplet from the upgoing vertical, and τ_c^k are chosen to displace the hydrophone response to the origin 'O' in figure 2.

To make this clearer and more concrete, we refer to figure 3, in which β is the rotation of the triplet

$$c\tau_c^{1j} = r \sin \beta,$$
$$c\tau_c^{2j} = r \sin(\beta - \gamma),$$
$$c\tau_c^{3j} = r \sin(\beta + \gamma),$$

where γ is 120 degrees ($\frac{2\pi}{3}$), and r is the radius of the circumscribing circle.

similarly

$$\alpha_c^{1j} = \sin \beta,$$
$$\alpha_c^{2j} = \sin(\beta - \gamma),$$
$$\alpha_c^{3j} = \sin(\beta + \gamma).$$

It is found that the second sum of equation 3 forms a cardioid shape, at a given frequency, which is almost independent of the rotation β. The magnitude of and reason for this variation are explained in annexes A and E. If we define this cardioid response

$$R_c(\phi, f) = \sum_{k=1}^{3} \alpha_c^{kj} \exp(\frac{2\pi}{c} f i(y_{kj} \sin \phi - c\tau_c^{kj})),$$

which is approximately the same for all cardioids, then equationresponse

$$r(\phi, f) = R_c(f, \phi) \sum_{j=1}^{N} \exp(\frac{-2\pi i f}{c}(x_j cos\phi - c\tau^j))$$

To *steer* this expression we take $c\tau^j = x_{kj} \cos \phi_0$, the second summation can then be written as $S(f, \phi, \phi_0)$ which is no more than the response for a linear array steered to ϕ_0.

The total response is then

$$r(f, \phi, \phi_0) = R_c(f, \phi) S(f, \phi, \phi_0)$$

It is worth noting that this is made up of two processes. The first R is formed on each of the individual triplets (first stage of processing). This means each triplet is beamformed into a cardioid response. These 'cardioid hydrophones' are then themselves beamformed as a linear array.

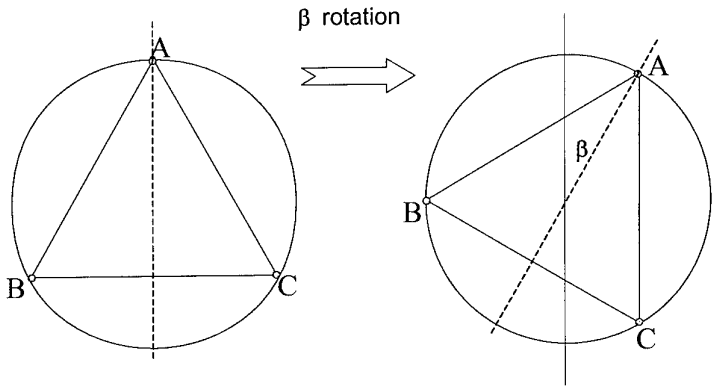

Figure 3 *The angle β shown for the array. It is assumed known for each of the triplets of the array allowing the (x, y, z) co-ordinates for the all hydrophones in the array to be known.*

Figure 4 shows some 2 dimensional beampatterns, for $\theta = \frac{\pi}{2}$, for a range of azimuthal steer angles. These plots have been calculated for a very short, 10 triplet, half-wavelength spacing between triplets, array so as to accentuate the effects as the look direction is steered away from broadside. All figures have been normalised to the same maximum value for ease of comparison. The polar plots are on a dB scale showing the maximum 30dB of response.

Figure 4a shows the beampattern for the broadside beam. It is clear that there is only one significant lobe. This is of course the very result that we require (in the standard linear array the ambiguous beam would be present pointing towards 270 degrees). We note that the first sidelobes are at approximately -13dB (as for the ambiguous array, with a constant shading function).

Figures 4(bcd) show the response as the look direction is steered progressively towards forward-endfire. As the look direction approaches endfire the beampattern becomes progressively more distorted. It is clear that in figure 4(d) the beampattern is very far from what one might desire. Furthermore, the maximum response of the beampattern is no longer in the nominal look direction. The reasons for these effects are twofold. Firstly, as for the ambiguous array, as we steer towards endfire the mainlobe beam becomes wider, in the ambiguous array we reach a point where the two ambiguous beams coalesce, in the directional array, however, the suppression

makes the coalesced beam appear skewed. The second, associated, effect is more subtle and we discuss it here in more detail.

Combination of beampatterns

Figure 5 shows a diagrammatic approach to understanding how the Centre's algorithm works. In figure (a) we have plotted the beampattern, on a log scale, of a single triplet in blue with its null in the 270 degree (starboard) direction. On the same figure we have plotted the response of a 10 element linear, ambiguous, array in blue. It has been steered to 45 degrees and shows, as expected, the ambiguous beam at 135 degrees. The cardioid array response is shown in b. This can be obtained by multiplying together the two responses of (a). (NB because the responses of figure (a) have been displayed on a log scale some care must be taken in moving from figure (a) to (b).)

This understanding of how the responses must be combined is the first step towards explaining the displaced beams at endfire. In figure c we show a blown up version of the responses for a beam nominally steered towards 5 degrees from endfire, but here not on a logarithmic scale. It is important to notice that the product of the two responses (in green) does not have its maximum at the maximum of either of the individual responses. This means that the overall cardioid array response maximum tends to skew away from endfire as shown in figure 5(c).

When the 3d algorithm is discussed in annex B it will be seen that again that algorithm gives skewed results towards endfire. There, however, it will be prudent to discuss the effect in terms of conflicting constraints. The underlying reason, however, is that as we approach endfire we progressively lose the x-direction extent, *i.e.* the array appears to be narrower and the ability to resolve to left and right is diminished. At endfire itself the system has no LR extent and consequently the system cannot be expected to work, regardless of algorithm used.

It is important to note that the algorithm as expressed above is a broadband algorithm despite the fact that it has been explained and discussed in terms of its individual frequency components. We can expect, however, that the gain achieved by the array is frequency dependent. This is not surprising since the directivity index of the array is frequency dependent. We shall not investigate this phenomenon here, other than to point out that the results of annex C can be used to quantify the response of the two algorithms detailed in this report in an analytic manner.

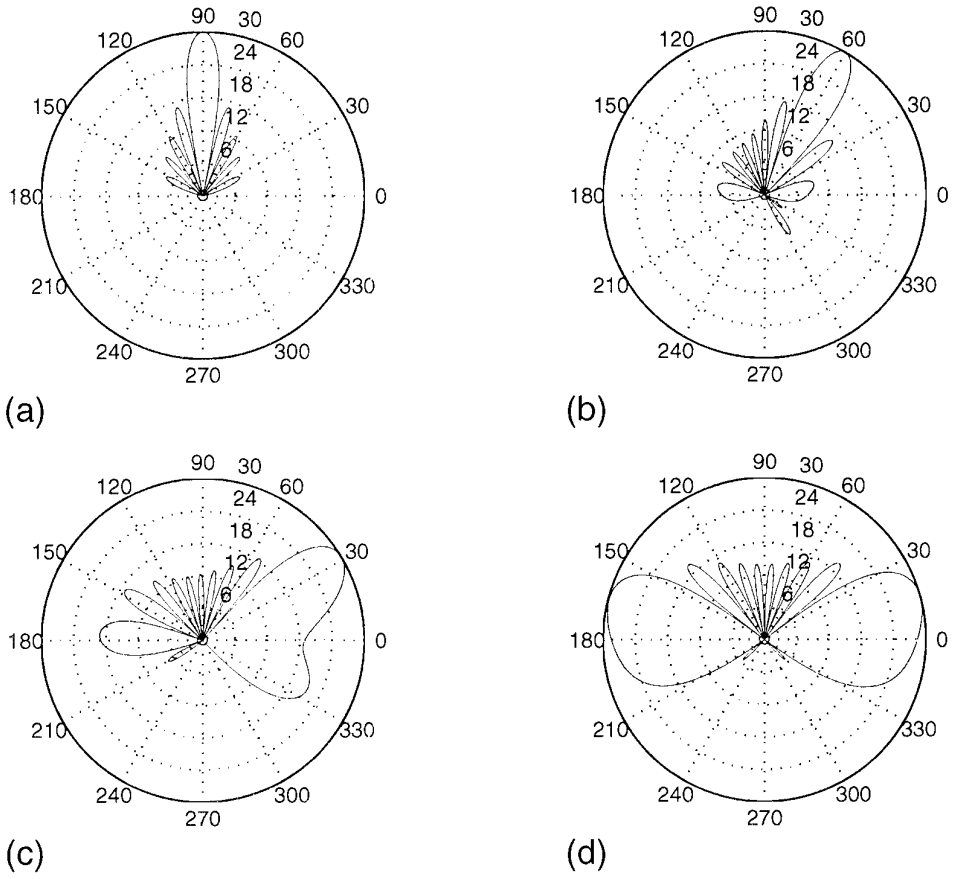

Figure 4 *Four 2-dimensional beampatterns for various steer directions in azimuth. As the beams are steered towards endfire the mainlobe becomes progressively distorted and eventually the maximum response is skewed away from the nominal steer direction. Steer angles are for (a), (b), (c) and (d) respectively: 90 (broadside), 60, 30 and 5 degrees.*

(a) (b)

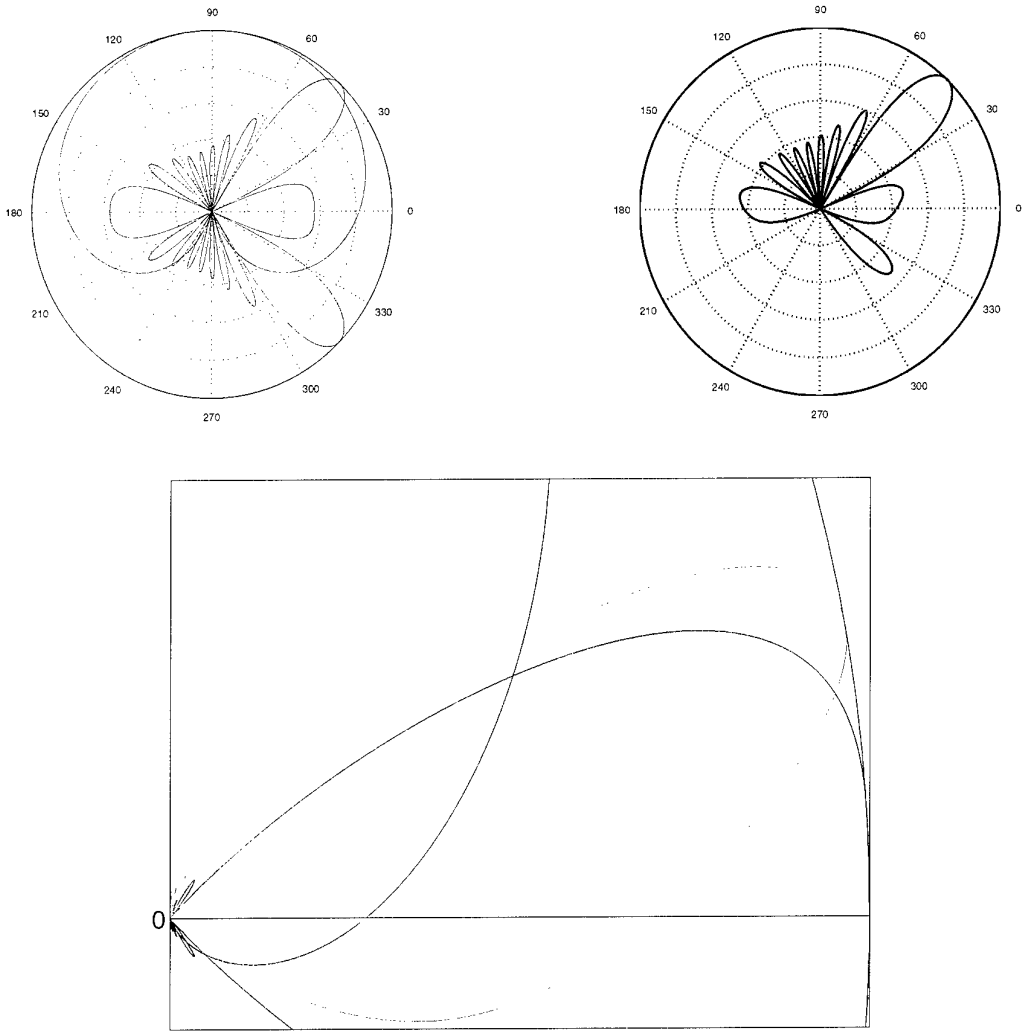

Figure 5 *Diagrammatic representation of how the Centre algorithm works. In (a) the ambiguous linear array response is shown in blue with the triplet 'shading' superimposed in red. (b) shows the response of an entire cardioid array with 10 triplets. (c) shows a blowup of a 10 triplet cardioid array steered to within 5 degrees off endfire. The red curve shows the single triplet response, the blue curve shows the broad beam formed by the ambiguous array with its maximum at the correct point. The product of these curves is the cardioid array response and is shown in green. It is clearly skewed away from endfire and has its maximum response at the wrong point (in actual fact at about 30 degrees off endfire).*

3

BACCHUS'98

In September of 1998 Saclant Undersea Research Centre held a joint trial with DERA (UK) using NRV Alliance. The trial, designated BACCHUS'98, had the primary objectives of evaluating ambiguity-resolving towed arrays; in particular comparing triplet and twin array technology. However, due to technical problems only a triplet array, provided by DERA was used to gather data during the trial. The array consisted of 120 hydrophones arranged into 40 triplets with a nominal upper operating frequency of 1780Hz.

DERA (UK) also provided the acoustic source for the experiment. The technology used was a free-flooded ring (FFR). The typical output power for the source was 220 dB re 1μPa. For the majority of the runs carried out a LFM sweep was used between 1100 and 1800 Hz with a duration of 3.5s. Indeed for all the data discussed in this report we only consider waveforms of this nature and infact will only process a 100Hz band between 1450 and 1550Hz.

The DERA free-flooded ring (FFR) broadband source was used which transmitted a LFM sweep between 1100 and 1700Hz over 3.0 seconds followed by a CW pulse at 1050Hz of 1.0 seconds duration.

No detailed information about conditions or statistical analysis of data is given in this report. This will be deferred to a subsequent report.

The majority of runs were of the type shown in figure 6 in which the target travels along a track for its image appears to take it through, beyond and back through a directional reverberation ridge which had previously been located on the Centre's SWAC series of sea trials. For a conventional array the target will become obscured as its images passes through the ridge. For the directional array, however, the ridge and target are separated to port and starboard so that the image remains unobscured for the whole run.

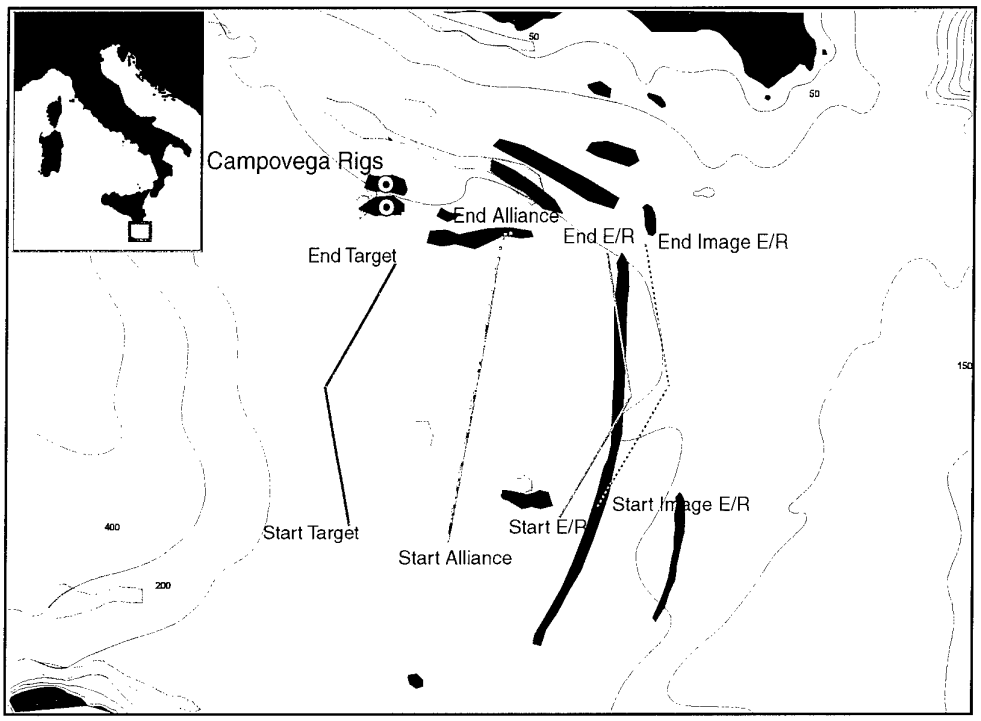

Figure 6 *A typical run from the Bacchus Trial of 1998. The main reverberation ridge running approximately North South was used for many of the runs since it provided a historically well known source of directional reverberation. In the case shown the NRV Alliance sails from South to North. An echo repeater and target proceed on the v-shaped courses as shown. The target's course is such that its ambiguous return appears to pass into, through and back through the reverberation ridge shown. The echo repeater is configured in such a way as to delay the return transmission so as to appear beyond the reverberation ridge. The Campovega Rig is also marked for completeness since it is observable in subsequent figures.*

4

Narrowband Processing of Real Data

The data from BACCHUS'98 is inherently broadband, and indeed the treatment of section 2 is appropriate to a system with significant fractional bandwidth. In this section, however, we shall give some indication of how the system works for a relatively narrowband data set.

The original hydrophone data is filtered to a band of 100Hz centred at 1500Hz. And then match-filtered. The algorithm of section 2 is used to beamform the data. At the same time we take one hydrophone from each of the triplets in the array to allow us to do traditional beamforming for comparison.

Since the thrust of this report is to detail and discuss cardioid algorithms rather than to give a detailed analysis of BACCHUS'98 data we have investigated only one representative run (run 15b) which is of the type described in the previous section. Similarly because we initially wish to consider and compare beamforming algorithms no normalization has been carried out.

The algorithm of section 2 was used. The twist angles were obtained from the non-acoustic data. The results obtained are not shown here. But it is important to state that the twist angles were extremely stable over the space of 10's of minutes. This implies at least for the short array under investigation here that the twist angles need not be measured very often.

When the beamforming is carried out it is over resolved at 1 degree intervals. (For independent beams the spacing is about 3 degrees at broadside). There are various reasons and consequences attendant on this decision.

i) because we are highly over-resolving at endfire the images for both the cardioid and linear beamforming will appear to be 'smeared out' in the endfire positions (0, ± 80 degrees).

ii) we have obviated the need to calculate the 3dB crossover points as we approach endfire. For the cardioid array this is a non-trivial matter since as was discussed in section 2 as we approach endfire the beams become skewed and no longer point in the nominal look direction.

Figure 7 shows the result for one ping from the ambiguous traditional array. We

have plotted both the port and starboard responses which are of course mirror images. 0 degrees indicates the tow direction Figure 8 shows the same set of data for the triplet array after cardioid processing. Negative angles indicate port whilst starboard angles are denoted by positive angles.

This ping shows various features of interest which are worth labouring. The main feature is the curved reverberation ridge which extends between 16 and 20km range and over all bearings. This feature can be associated with the long reverberation ridge shown in figure 6 and discussed at some length in the previous section. After cardiod processing it has been resolved to starboard (in agreement with figure 6!).

At a range of approximately 13.5km a distinct very bright bottom feature can be discerned. After cardioid processing we see that the feature is found physically on the starboard.

At a range of 24.5km towards forward end-fire a bright feature can be seen. This is expected to be the Campovega Rig, and after cardioid processing this hypothesis is further substantiated by the fact that it lies to port (in agreement with figure 6).

One further feature of interest is the other-ship noise which can be seen as a prominent vertical line at all ranges. After processing this line has been resolved to starboard. This brings out the interesting point that because left-right resolution is being carried out on receive the system can also operate in a passive mode. (As opposed to left-right resolution methods which attempt to resolve on transmit).

Figure 9 makes these ideas rather more concrete and gives a more quantitative measure of the left-right suppression achievable with the beamforming for this particular system. It shows three A-scans, of the Campovega Rig, the reverberation ridge and of the bright bottom feature. The suppression on the bottom feature is about 10dB and for the Campovega Rig it is 13dB. On the reverberation ridge a quantitative measure is harder to assess but it is clear that the overall shape of the ridge has disappeared (been significantly suppressed) on the port side of the display.

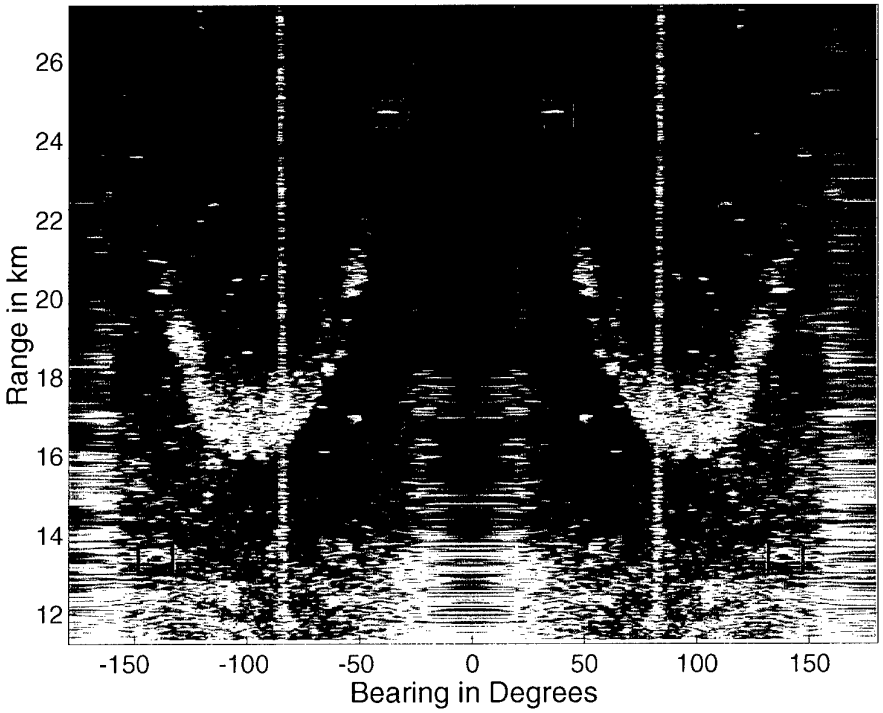

Figure 7 *B-scan for non-directional array. The display has been plotted over the whole range of angles, both port and starboard to facilitate comparison with figure 8. The boxed bright spots at a range of approximately 25km is the Campovega Rig. The boxes at 13.5km highlight a bright bottom feature. The vertical line at ±180 degrees is other passive ship noise.*

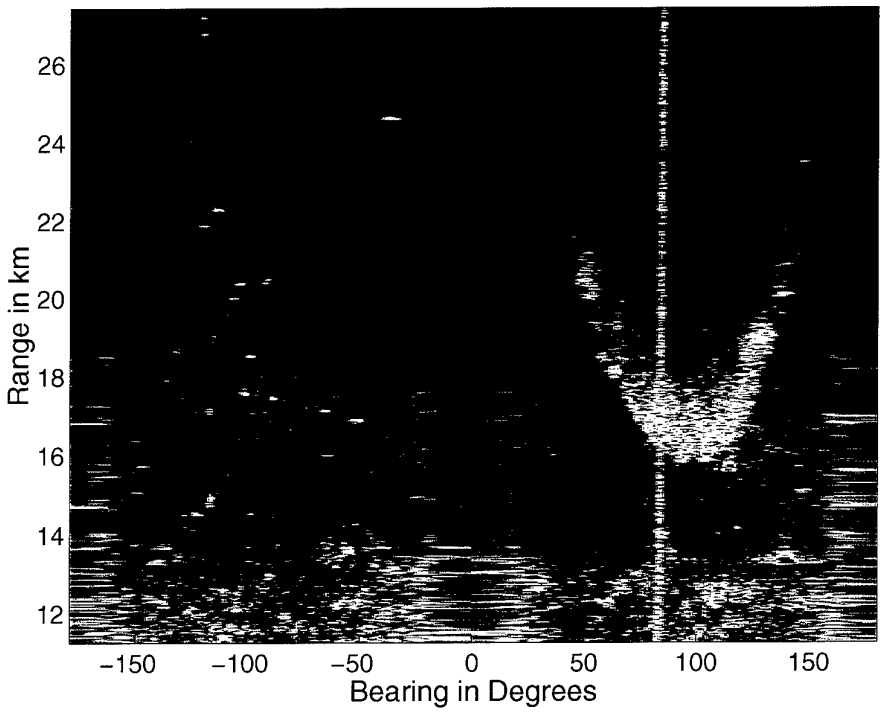

Figure 8 *B-scan for directional array. In this display it is clear that the Campovega Rig is on the port side and the reverberation ridge and the other-ship noise have been resolved to starboard in agreement with figure 6.*

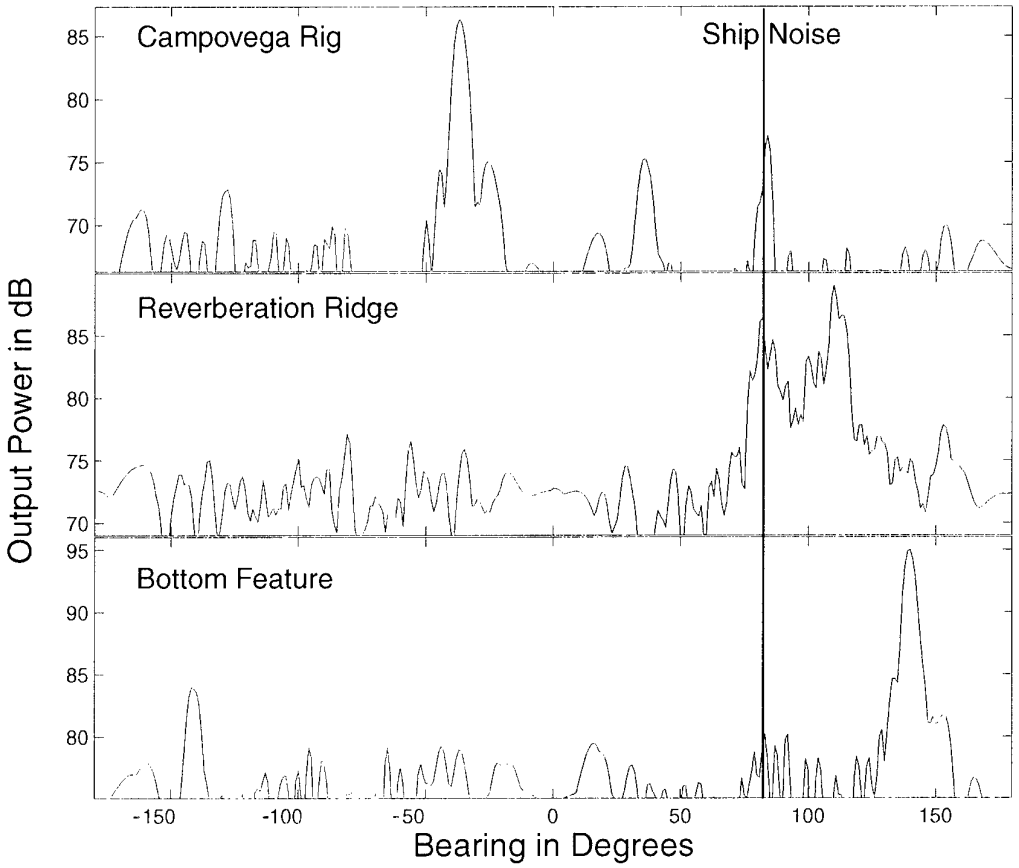

Figure 9 *A-scans of three representative points taken from the B-scan of figure 8. The upper trace exhibits the Campovega Rig which shows a suppression of approximately 12dB between port and starboard. In the middle scan the reverberation ridge can be seen to have been suppressed on the port side. In the bottom scan the bright bottom feature can be seen to have been suppressed by approximately 10dB. (Note the ordinate scale is different for the three displays)*

5

Conclusions

The main purpose of this report is the documentation of the proposed cardioid algorithm which is to be used by the Saclant Undersea Research Centre. Consequently, some effort has been expended in detailing the algorithm and quantifying some of its particular properties. The appendices have been used to tabulate the analytic expressions for SNR and left-right suppression.

We have taken the opportunity, however, to describe and compare a '3d-algorithm'. We have shown how the '3d-algorithm' gives superior left-right suppression but the 'Centre algorithm' gives superior SNR performance in uncorrlated noise.

It is recommended that this work should be further verified and extended by application to more data. In particular the application of the cardioid algorithms to

1. investigate the difference in left-right reverberation statistics. A directional array gives an investigator a unique opportunity to compare, for instance, the difference between the characteristics of upslope and downslope reverberation statistics.

2. Being broadband the algorithm allows the investigation of not only left-right comparisons but also the processing of different bands. For instance the Bacchus data (section 3) although only 600Hz wide is known to show very different performance for the upper and lower bands [4]. It is highly recommended that these effects should be further investigated and quantified as an initial indicator for the Mercury trial of 1999.

Annex A
Real Weights

In section 2 we used a real weighting on each of the individual triplet hydrophones which was proportional to the projection of the hydrophones position vector onto the horizontal. We did this because of limitations in the Centre's real time beamformer. In this annex we discuss the approximations inherent in this approach.

If we consider a single triplet and impose the following constraints

$$\mathbf{w^H c_1} = 1 \tag{4}$$

where $\mathbf{c_1}$ is the steering vector defining the look direction and $\mathbf{w}$ is the weight vector that we wish to calculate. For the triplet this lies in the horizontal, in the plane of the triplet and the actual direction defines whether our beamformed cardioid is looking left or right. We also impose

$$\mathbf{w^H c_2} = 0 \tag{5}$$

$\mathbf{c_2}$ is the steering vector for the opposite direction to the look direction and as such defines the null in our beampattern.

These two constraints can be written more succinctly as

$$\mathbf{C^H w} = \mathbf{b} \tag{6}$$

with

$$\mathbf{C} = [\mathbf{c_1 c_2}] \text{ and } \mathbf{b} = [\mathbf{1}, \mathbf{0}]^{\mathbf{T}}$$

Furthermore, let us define,

$$\mathbf{w^H w} = 1,\ \mathbf{{c_1}^H c_1} = 1.0,\ \mathbf{{c_2}^H c_2} = 1.0,$$

for mathematical convenience.

Assuming that noise is uncorrelated between the triplet hydrophones, the optimum set of weights, *i.e.* which maximises the SNR, is given by.[6]

$$\mathbf{w_{opt}} = \mathbf{C}(\mathbf{C^H C})^{-\mathbf{1}}\mathbf{b}. \tag{7}$$

Which after some rearrangement becomes:

$$\mathbf{w_{opt}} \propto \mathbf{c_1} - \alpha^* \mathbf{c_2}, \tag{8}$$

where $\alpha = \mathbf{c_1^H c_2}$ is the correlation between the vectors $\mathbf{c_1}$ and $\mathbf{c_2}$. It is interesting to note that if $\mathbf{c_1}$ and $\mathbf{c_2}$ are orthogonal the optimum weight is no more than the steering vector (the usual case in beamforming). We shall return to these considerations again in annex C where this term plays a crucial role in the signal to noise ratio gain of the system.

At this stage it is helpful to consider the individual terms of the above expression

$$\mathbf{w_{opt}} = \frac{1}{\sqrt{3}} \begin{bmatrix} e^{-2\pi a i \sin\beta} \\ e^{-2\pi a i \sin(\beta-\gamma)} \\ e^{-2\pi a i \sin(\beta+\gamma)} \end{bmatrix} - \frac{\alpha^*}{\sqrt{3}} \begin{bmatrix} e^{2\pi a i \sin\beta} \\ e^{2\pi a i \sin(\beta-\gamma)} \\ e^{2\pi a i \sin(\beta+\gamma)} \end{bmatrix}. \tag{9}$$

For the triplet we can write

$$\alpha^* = \frac{1}{3}(e^{-4\pi a i \sin\beta} + e^{-4\pi a i \sin(\beta-\gamma)} + e^{-4\pi a i \sin(\beta-\gamma)}).$$

If the parameter a, which is the radius of the circumscribing radius of the triplet in units of wavelength, is small we can make expansions to *first order* in a.

$$\alpha^* = \frac{1}{3}(3 - 4\pi a i(\sin\beta + \sin(\beta-\gamma) + \sin(\beta-\gamma)). \tag{10}$$

Now, we note that, from annex F

$$\sin\beta + \sin(\beta-\gamma) + \sin(\beta+\gamma) = 0.0$$

so that

$$\alpha^* = 1.0$$

then

$$\mathbf{w_{opt}} = \frac{1}{\sqrt{3}} \begin{bmatrix} e^{2\pi a i \sin\beta}(1 - (1 + 4\pi a i \sin\beta)) \\ e^{2\pi a i \sin(\beta-\gamma)}(1 - (1 + 4\pi a i \sin(\beta-\gamma)) \\ e^{2\pi a i \sin(\beta+\gamma)}(1 - (1 + 4\pi a i \sin(\beta+\gamma)) \end{bmatrix} \tag{11}$$

and finally

$$\mathbf{w_{opt}} \propto \begin{bmatrix} \sin\beta \\ \sin(\beta-\gamma) \\ \sin(\beta+\gamma) \end{bmatrix} \odot \begin{bmatrix} e^{-2\pi a i \sin\beta} \\ e^{-2\pi a i \sin(\beta-\gamma)} \\ e^{-2\pi a i \sin(\beta+\gamma)} \end{bmatrix} \tag{12}$$

where $\odot$ is the element-by-element product operator.

We have, then, that the optimum weights for the triplets with the given constraints have the effect of delaying the signal to the centre of the circumscribing circle of the triplet (given by the exponential phase terms) and real weights which are in the following ratio

$$\frac{|w_1|}{\sin\beta} = \frac{|w_2|}{\sin(\beta-\gamma)} = \frac{|w_3|}{\sin(\beta+\gamma)}. \tag{13}$$

At this point it is worth stressing that although the above calculation has been carried out as a narrowband calculation the final result for the optimum weights for a broadband signal is made up of a set of delays and real weights which are independent of frequency, assuming that the small a expansion is valid for at all points in the band. Consequently the result holds across any band of interest. The observant reader, however, will have noticed that the small term expansions carried out above have not been carried out completely *i.e.* we have retained all powers of a in the delay term of equation 11. The reason for this is that we wish to find an explanation and justification for the expression for the triplet weights given in section 2.

Annex B

Alternative Narrowband Approach

In the main body of the text we have constrained our prospective algorithm to be composed of two stages, the first an initial beamforming at the triplet level. The second a 'traditional' steering of the array using these new 'directional hydrophones'. This approach is, to a certain extent, imposed on us by the structure of Saclant Centre's real-time system.

If we, however, consider the entire array as a 3d beamformer and limit ourselves to narrowband systems the choice of algorithms becomes substantially widened.

In this section we shall simply state an obvious narrowband algorithm. We shall, however, return to it in more detail when we are considering some of the signal-to-noise ratio properties of the two algorithms.

With the freedom offered by the full three dimensional nature of the array the most obvious approach is to impose the following constraints, using the notation of annex A:

$$\mathbf{c_1^H w} = 1$$
$$\mathbf{c_2^H w} = 0$$

with, $\mathbf{c_1}, \mathbf{c_2}$ representing the vectors which point in the look direction and the null direction respectively. Here we are interested in the situation where the null direction is in the ambiguous direction to the look direction and in the same plane. As usual we define the constraint vectors such that $|\mathbf{c_1}|^2 = 1$ and $|\mathbf{c_2}|^2 = 1$. Now, however, these vectors contain $3N$ elements where N is the number of cardioids. We combine the two vector constraints into one matrix constraint:

$$\mathbf{C^H} = \mathbf{b} \tag{14}$$

where

$$\mathbf{C} = [\mathbf{c_1 c_2}], \quad \mathrm{b} = [1\ 0]^{\mathrm{H}}$$

If we take the pseudo-inverse we find, after some arrangement, the following solution for $\mathbf{w}$ analagous to that given in annex A:

$$\mathbf{w} = \frac{\mathbf{1}}{\mathbf{1} - |\alpha|^{\mathbf{2}}}(\mathbf{c_1} - \alpha^* \mathbf{c_2}) \tag{15}$$

where $\alpha = \mathbf{c_1^H c_2}$ is the correlation between the vectors $\mathbf{c_1}$ and $\mathbf{c_2}$.

Annex C

Signal to Noise Ratio Considerations

In this annex we will point out some of the signal to noise properties of the algorithms described in the body of the main text and the 3-dimensional approach of annex B. For both of the algorithms we shall consider the signal gain, the uncorrelated noise gain and the correlated noise gain.

We begin by considering the performance of the two algorithms in uncorrelated noise. This is the noise that we associate typically with electronic noise in the system. There is also a component of flow noise which can be modelled as uncorrelated even within a triplet.[7]

Next the performance of the two algorithms is analysed in correlated noise which provides a model of sea-noise. It is worth noting that the performance of the algorithm in 'directional noise' is best considered in terms of left-right suppression which is addressed in annex D.

Signal to Uncorrelated Noise for Centre Algorithm

For the Centre algorithm we shall assume that the triplets are not rotated. It is shown in annex E that the overall response of the triplet remains fairly constant with rotation so that the results found here are general. We shall only consider signals arriving in the horizontal plane. This is of course an approximation since in a real sonar system we may expect returns from above or below horizontal. We shall consider the signal and the noise output powers separately.

Signal Component

For a general plane-wave signal on the horizontal coming from an azimuthal angle of ϕ the response is given by:

$$\frac{1}{\sqrt{N_c}} \sum_{j=1}^{N_c} C_j \sum_{i=1}^{3} C_i^c \exp(2\pi i(asin\bar{\gamma}_i - x_j \cos\phi - y_i \sin\phi)) \tag{16}$$

where C_j represents the complex weight for the steering in azimuth, C_i^C is the real cardioid weight, $\bar{\gamma}_i$ is the rotation of the particular hydrophone i, within the triplet, from the normal. It is clear after a little thought that

$$y_i = a \sin\bar{\gamma}_i.$$

And so after some manipulation we can write the response as

$$\sqrt{N_c}\sum_{i}^{3}\sin\bar{\gamma}_i\exp(2\pi ai\sin\bar{\gamma}_i(1-\sin\phi)). \tag{17}$$

Since we assume that no rotation has taken place $\sin\bar{\gamma}_1 = 0$, $\sin\bar{\gamma}_2 = \frac{\sqrt{3}}{2}$ and $\sin\bar{\gamma}_3 = \frac{-\sqrt{3}}{2}$. So that we can write the output as

$$i\sqrt{3N_c}\sin\sqrt{3}\pi a(1-\sin\phi)$$

and the output signal power is

$$\text{Output Signal Power} = 3N_c\sin^2(\sqrt{3}\pi a(1-\sin\phi)). \tag{18}$$

With broadside at $\phi = \frac{-\pi}{2}$.

Uncorrelated Noise component for Centre Algorithm

Calculation of the noise output power is similarly straightforward although it can only be expressed in a statistical manner. The expectation of the output power is

$$E\left(\sum_i\sum_{i'}\sum_j\sum_{j'}C_jC_{j'}C_i^CC_{i'}^Cn_{ij}n_{i'j'}\right) \tag{19}$$

where n_{ij} represents a noise sample on the ith hydrophone of the jth triplet.

$$= \sum_i\sum_{i'}\sum_j\sum_{j'}C_jC_{j'}C_i^CC_{i'}^C\delta_{i,j}\delta_{i',j'}$$

$$= \sum_i\sum_j|C_j|^2|C_i^C|^2.$$

But on using the explicit values for these parameters and using the results of appendix F we obtain

$$\text{Noise Output Power} = 1.5,$$

and finally we can write

$$\text{Output Signal to Noise Ratio} = 2N_c\sin^2(\sqrt{3}\pi a(1-\sin\phi)) \tag{20}$$

This result, as it stands is far from self-explanatory so some comments are worthwhile.

(i) This result has been calculated for two hydrophones on the horizontal. When their horizontal spacing is $\frac{\lambda}{4}$ the Output Signal to Noise Ratio (which in this case is

the gain of the system) for a signal from broadside is $2N_c$. This compares with the $3N_c$ we would usually expect for a system with $3N_c$ hydrophones. This is because, in effect one of the hydrophones has been turned off.

(ii) as a decreases the signal to noise ratio also falls. The reason for this is due to the decrease in signal rather than any change in noise output power. As an order of magnitude indication if we assume that $a = 0.05\lambda$ as a typical value then the output SNR at broadside is $2N_c$ 0.27. A loss of almost 6dB over the $\frac{\lambda}{4}$ case.

(iii) As the look-direction is steered from broadside the output signal to noise ratio decreases. If we take the loss of output signal to noise ratio at endfire compared to that at broadside we get;

$$SNR_{loss} = \frac{\sin^2(\sqrt{3}\pi a)}{\sin^2(2\sqrt{3}\pi a)} \tag{21}$$

For small values of a this ratio becomes a factor of a quarter or in otherwords there is a loss of 6dB as we steer from broadside to endfire.

(iv) It is worth noting that the expression 20 above when plotted out actually has the cardioid shape over the entire range of ϕ. In practice, of course, only one half of the range of angles is used since an alternative set of weights would be used to look on the opposite side of the array.

Signal to Uncorrelated Noise for 3d Algorithm

We saw in annex B how the optimum weight vector for the 3d algorithm can be written as

$$\mathbf{w} \propto \mathbf{c_1} - \alpha^* \mathbf{c_2}$$

We ignore the constant of proportionality in what follows since we are ultimately interested in ratios.

$\mathbf{w}$ is the weight vector matched to a signal coming from the direction given by $\mathbf{c_1}$. A signal of unit power can be represented, therefore, as $\sqrt{M}\mathbf{c_1}$ where $M = 3N_c$ is the total number of sensors. The output signal power then is given by

$$P = M|\mathbf{w_1^H c_1}|^2 = M(1 - |\alpha|^2)^2.$$

For such a system the output uncorrelated noise power, covariance matrix $R_N = I$ is

$$\mathbf{w^H R_N w} = \mathbf{w^H I w} = \mathbf{w^H w} = \mathbf{1} - |\alpha|^2. \tag{22}$$

Then the output signal-to-noise ratio is

$$\mathrm{SNR}_{\mathrm{out}} = M(1 - |\alpha|^2) \tag{23}$$

It is interesting, then, to ask the questions how does this algorithm perform at broadside and as we steer towards endfire. We wish to do this ultimately of course with reference to the Centre algorithm discussed above.

At broadside then we can write, expanding up to powers of a^2

$$M(1 - |\alpha|^2) = 3N_c(8\pi^2 a^2)$$

where we have used the results of annex F.

But, referring to equation 23 and expanding it to the second order in a we see that the signal to noise ratio at broadside is equal for the two algorithms. This is as expected since, at broadside, the 3d-algorithm forms a cardioid on each triplet.

Away from broadside we can write generally that

$$3\alpha = \mathbf{c_1^H c_2} = exp(4\pi \sin\bar{\gamma}_1 \sin\phi + 4\pi \sin\bar{\gamma}_2 \sin\phi + 4\pi \sin\bar{\gamma}_3 \sin\phi) \tag{24}$$

Again using expansions up to second order

$$\alpha \approx 1 - 4\pi^2 a^2 \sin^2\phi$$

so that, the uncorrelated SNR is

$$M(1 - |\alpha|^2) \approx 3N_c(8\pi^2 a^2)\sin^2\phi$$

It is clear then that the 3d-algorithm has an inferior performance with regard to uncorrelated signal-to-noise ratio at all angles steered off broadside.

Performance of Center Algorithm in Correlated Noise.

When we come to consider how algorithms behave in the presence of correlated noise expressions rapidly become complicated and unilluminating. However, we shall consider the Centre algorithm in some detail since it represents a crucial measure for real experimental systems.

We assume the narrowband approximation for the covariance matrix:

$$R_N = \begin{pmatrix} 1 & f & f \\ f & 1 & f \\ f & f & 1 \end{pmatrix} \tag{25}$$

where

$$f = \frac{\sin(2\pi\bar{a})}{2\pi\bar{a}}$$

and $\bar{a} = \sqrt{3}a$ is the distance between hydrophones. The noise output power then for one triplet is $w^H R_N w$ which can be written as

$$(1-f)w^H I w + f w^H \begin{pmatrix} 1 & 1 & 1 \\ 1 & 1 & 1 \\ 1 & 1 & 1 \end{pmatrix} w. \tag{26}$$

The second term can be shown to be $9\pi^2 a^2 f$. Consequently,

$$\text{Signal to correlated noise power per triplet} = \frac{(1-|\alpha|^2)}{1.5(1-f)+9\pi^2 a^2 f}. \tag{27}$$

But, taking series expansions to a^2,

$$f = \frac{\sin(2\pi\bar{a})}{2\pi\bar{a}} = 1 - \frac{3(2\pi a)^2}{3!}$$

and

$$(1-f) = \frac{(2\pi a)^2}{2}.$$

Now if we ignore the intertriplet correlation then we can just scale this result by the number of triplets N_c.

$$\text{Signal to correlated noise power for array} = \frac{3N_c}{4}(1-\sin\phi)^2 \tag{28}$$

for small a.

In reality of course the overall signal to noise ratio at the output is an appropriately weighted combination of correlated and uncorrelated SNR's.

Performance of 3d-Algorithm in Correlated Noise

The analysis of the correlated noise for the 3d-algorithm is very similar to that for the Centre algorithm and it is easily shown that after only including terms up to a^2 that the

$$\text{Signal power} = 3N_c(8\pi^2 a^2 \sin^2\phi). \tag{29}$$

$$\text{Correlated Noise power} = 8\pi^2 a^2 \sin^2\phi. \tag{30}$$

so that

$$\text{Signal to correlated noise power for array} = 3N_c. \tag{31}$$

This final expression needs some comment. It appears that the array is now giving a gain of $3N_c$ i.e. the gain that would have been achieved, against uncorrelated noise, if we had used all of the hydrophones in a linear configuration but now we have gained the ability to discriminate between left and right. We have seen however, that both the algorithms discussed have relatively poor performance, against uncorrelated noise. The choice of whether to use one of the algorithms discussed here or to use a linear array subset (which is always available by taking one element from each triplet) is always open to the sonar operator. However, the actual operating conditions under which a triplet algorithm should or should not be used is still to be investigated.

Also in any comparison between directional and 'ordinary' processing it is important to realise that the two approaches differ at a very basic level. Simplistically, for ordinary processing we add signals, for the directional processing discussed above signals are subtracted. In the preceding discussions this has caused no problems because the approach has been analytic. However, in reality, such systems will be limited by the number of bits being used in the calculations.

Annex D

Left-Right suppression

We can easily calculate the expected left-right suppression for the two algorithms which have previously been called the '3d-algorithm' and the 'Centre-algorithm'. When we talk about left-right suppression here we are interested in suppression of a signal assuming that it can be modelled by a plane wave.

Centre Algorithm

We can use equation 18 in annex C to calculate the left-right suppression for the Centre algorithm.

The output power for a signal with a look direction given by an azimuthal angle of ϕ is

$$3N_c \sin^2(\sqrt{3}\pi a(1 - \sin\phi)),$$

the output power for a signal from the ambiguous direction $(180 + \phi)$ is

$$3N_c \sin^2(\sqrt{3}\pi a(1 + \sin\phi))$$

So that the left-right suppression is approximately,

$$\frac{(1 - \sin\phi)^2}{(1 + \sin\phi)^2} \quad \frac{-\pi}{2} \leq \phi < \frac{\pi}{2}. \tag{32}$$

The dashed lines of figure 10 shows the theoretical left right suppression as a function of ϕ. It clearly has the correct overall form with suppression falling from, nominally an infinite value at broadside to 1 at endfire where no left-right discrimination is possible for the cardioid.

The crosses show the values taken from experimental data taken from trial BAC-CHUS'98. 40 pings have been analysed choosing objects which appear point-like on a b-scan display. The suppression between right and left is measured and displayed as a star on figure 10. A dense cluster of returns can be seen at 140 degrees. This is the Campovega Rig, which for the 40 pings investigated is always visible with a large signal to noise ratio, It is important to note that the dashed line of figure 10 represents a maximum suppression. Reasons why this may not be achieved include;

(i) physical mismatches in the equipment such as errors in the roll sensors, phase and amplitude errors in the hydrophones, bandwidth effects (we treat 100 Hz band as narrow band).

(ii) Channel effects. Any physical mechanism which stops the return from a point like object looking like a plane wave at the array may degrade the performance (although it is conceivable that they will improve the performance in some situations).

(iii) If another object really can be found in the ambiguous direction the suppression may be significantly less than expected. By the same argument the maximum suppression that can be expected even in a noise-limited environment is no more than the signal to noise ratio since even when the ambiguous return is pushed below the noise the ambiguous return will be equivalent to the noise level.

3d-Algorithm

Theoretically the left right suppression is always infinite, since the constraint in the ambiguous direction is chosen to be zero. In reality of course there will be leakage due to errors (see annex E) and the signal will not come entirely from the horizontal, or indeed from one particular azimuthal direction.

In figure 11 the measured suppression is shown for the 3d-algorithm. The notation used is as for the Centre algorithm. Here we have retained the theoretical dashed curve for the Centre algorithm to aid the reader. It is clear that the measured results often exceed the Centre algorithm indicating that the 3d-algorithm exhibits superior performance. Again the Campovega Rig returns can be seen forming a cluster at 140 degrees but now showing a suppression of about 20dB.

Figure 12 is included for completeness, and should ideally be compared with figure 9. The suppression of the bottom feature and the Campovega Rig is such that no indication of the strong features remain above the noise floor.

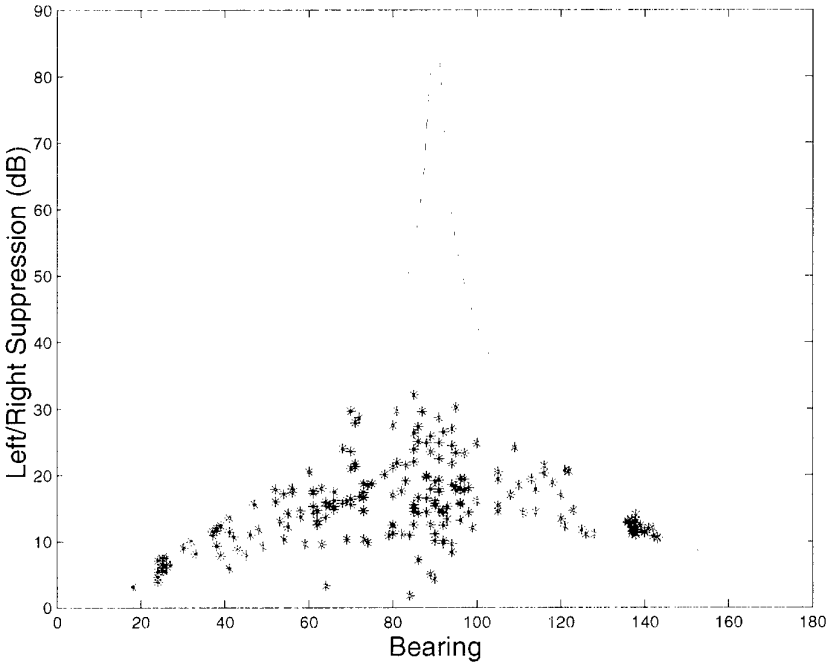

Figure 10 *Theoretical and Experimental values for Left-Right suppression for the Center algorithm is used. Only small targets with large SNR's were investigated over 40 pings of data. The crosses show the experimentally measured values of SNR. The dashed line indicates the theoretical maximum given by equation 32*

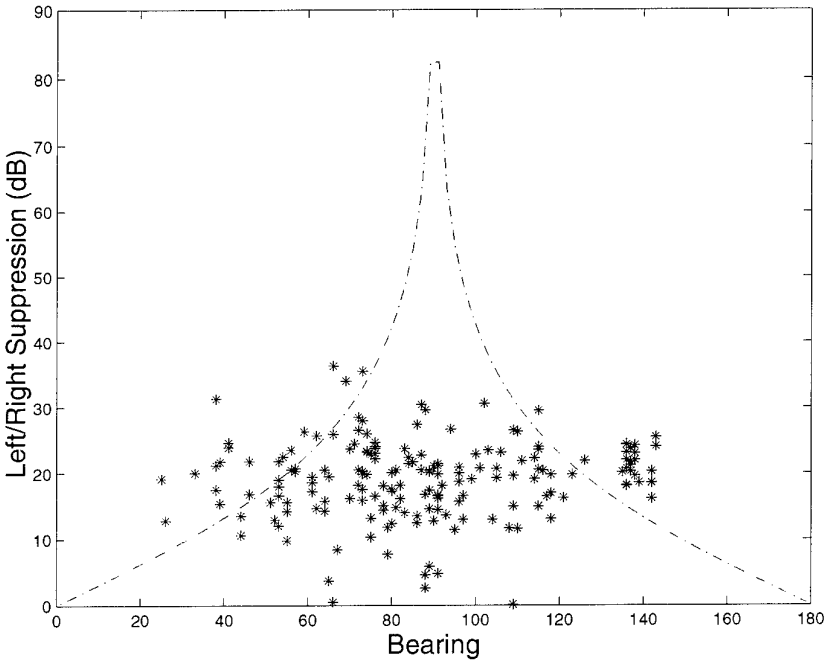

Figure 11 *Experimental values for Left-Right suppression for the 3d algorithm. The dashed line shows the theoretical limits for the Centre algorithm it is clear that for a range of look directions the 3d algorithm is superior in terms of suppression.*

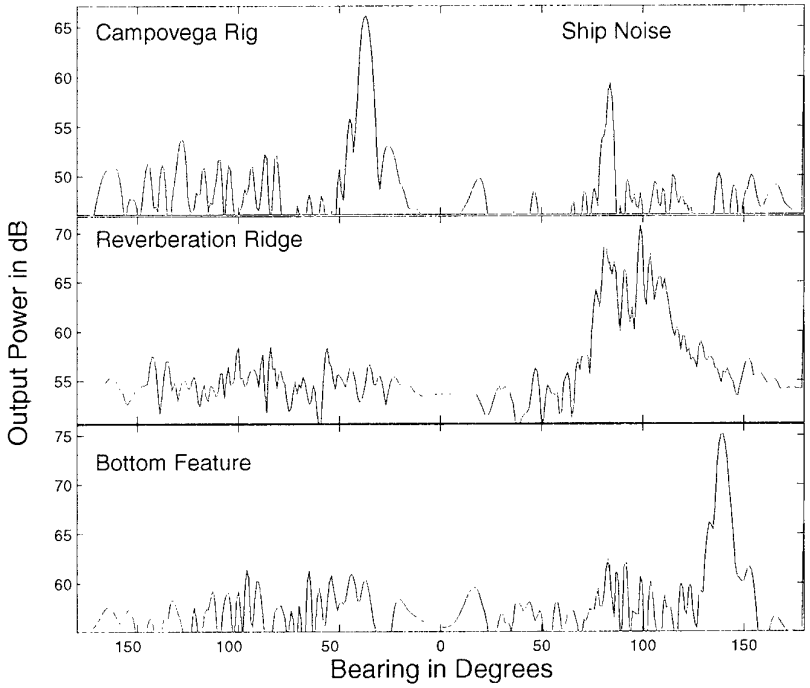

Figure 12 *A scans of three representative points for the same data set as used in figure 9. The upper display shows the results for the Campovega Rig, the middle scan shows the Reverberation ridge and the bottom scan shows a bright bottom feature. In distinction to figure 9 the suppression of the objects is down into the noise floor regardless of angle. This is the same effect as has been exhibited more quantitatively in figure 11. (Note the change of ordinate scale between the three displays).*

Annex E

Error Considerations

The first 'error' that we shall address is that of twist on the sensors on the array. It was shown in annex A that the algorithm described in section 2 was an approximation. The consequence of the approximation is that for any particular triplet the response, although always being a maximum in the horizontal, will vary in magnitude with twist angle even if this value is known exactly. If this variation were large the effect on the beamforming could be serious since each triplet would have a different gain. We test this effect 'empirically' by calculating the beampatterns for a single triplet for a range of twist angles for a system operating at 3400 Hz and a triplet with radius 0.027m. Figure 13 shows the response of a triplet as the twist angle (β in figure 3) is varied. The response is taken on the horizontal and is displayed in dB. Only angles between 0 and 60 degrees are shown since the response repeats every 60 degrees. It is clear that the response variation is small (about 0.4dB). For lower frequencies the variation is expected to be less (a would be smaller in equation 11).

However, in the real system, we also expect an error to be associated with the twist angle (we use β but the actual value is β'). The reasons for this are clear, there may be an error in the twist sensor itself or since we interpolate between twist sensors to find the twist at individual triplets an extra error may be introduced.

We ask the question then, what is the response in the horizontal in the null and the look direction for an individual triplet rotated to β' if the actual rotation is β. It is important to note that these are not necessarily the minimum or maximum response for the whole cardioid response.

The actual steering vector for a signal coming from the nominal null direction is, ignoring normalization terms,

$$\mathbf{s} = [e^{2\pi a i \sin\beta}, e^{2\pi a i \sin(\beta-\gamma)}, e^{2\pi a i \sin(\beta+\gamma)}] \tag{33}$$

The weights used are

$$\mathbf{w} = [\sin\beta' e^{2\pi a i \sin\beta'}, \sin(\beta'-\gamma) e^{2\pi a i \sin(\beta'-\gamma)}, \sin(\beta'+\gamma) e^{2\pi a i \sin(\beta'+\gamma)} \tag{34}$$

Consequently, the response is, after taking note of the fact that a is small and making the appropriate expansions

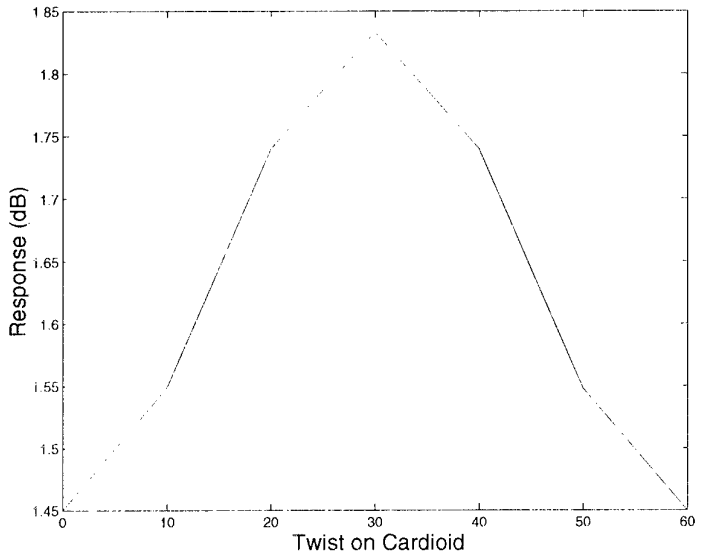

Figure 13 *The maximum response of a triplet after using the algorithm of section 2 plotted against known twist angle (in degrees). The maximum response is always in the horizontal. The operating frequency is taken at 3400Hz (as opposed to the 1500Hz of section 4) for a triplet radius of 0.027m.*

$$\begin{aligned}\mathbf{w^H s} \quad \propto & \sin\beta'(\sin\beta - \sin\beta') + \sin(\beta' - \gamma)(\sin(\beta - \gamma) - \sin(\beta' - \gamma)) \\ & + \sin(\beta' + \gamma)(\sin(\beta + \gamma) - \sin(\beta' + \gamma))\end{aligned} \tag{35}$$

and using the results of section F

$$\mathbf{w^H s} \propto (1 - \cos(\beta - \beta')) \tag{36}$$

and if the error is small

$$|\mathbf{w^H s}|^2 \propto (\beta - \beta')^4 \tag{37}$$

In the nominal look direction a similar treatment gives

$$\mathbf{w^H s} \propto (1 + \cos(\beta - \beta')) \tag{38}$$

We make no further comment on these analytic expressions at the moment, other than to note that empirically the errors associated with the twist sensors seem to be relatively unimportant.

Phase errors

We now carry out a similar treatment for phase errors. These errors may have two cause: system errors (e.g. badly matched hydrophones) or signal processing effects. In the broadband processing the phases are applied as delays produced by an interpolation filter, discretization errors in the delays will equate to phase errors in the frequency domain. We expect the second, signal processing, effect to be dominant so we shall associate the errors with the weights applied.

We assume phase errors $(\delta_1, \delta_2, \delta_3)$ on the hydrophones of the triplet. These vary from sample to sample and are zero mean. We also expect that each is uniformly distributed; although this will not be used in what follows. The steering vector is

$$\mathbf{s} = [e^{2\pi a i \sin\beta}, e^{2\pi a i \sin(\beta-\gamma)}, e^{2\pi a i \sin(\beta+\gamma)}] \tag{39}$$

the weights applied are

$$\mathbf{w} = [\sin\beta e^{2\pi a i \sin\beta+\delta_1}, \sin(\beta-\gamma)e^{2\pi a i(\sin(\beta-\gamma)\delta_2}, \sin(\beta+\gamma)e^{2\pi a i \sin(\beta+\gamma)+\delta_3}] \tag{40}$$

when a is small

$$\mathbf{w^H s} \propto \sin\beta\delta_1 + \sin(\beta-\gamma)\delta_2 + \sin(\beta+\gamma)\delta_3 \tag{41}$$

but the δs are random variables with zero mean so we should deal with expectations

$$E(\mathbf{w^H s}) = 0 \tag{42}$$

but more importantly, if we assume

$$E(\delta_i \delta_j) = \sigma^2 \delta_{ij} \tag{43}$$

where δ_{ij} is the kronecker delta. After using results from annex F, we find

$$E(|\mathbf{w^H s}|^2) = 1.5\sigma^2 \tag{44}$$

Annex F
Some Useful Expressions

For ease of use we state some of the formulae which have been used at various points throughout this report. We are concerned with expressions in which three terms are summed, one from each of the sensors on the triplet. We shall use the same notation as throughout the report where γ is 120 degrees ($\frac{2\pi}{3}$ radian), the angular separation between the sensors in the triplet.

Some tedious algebra gives us

Result 1

$$\sin\beta\sin\beta' + \sin(\beta-\gamma)\sin(\beta'-\gamma) + \sin(\beta+\gamma)\sin(\beta'+\gamma) = \frac{3}{2}cos(\beta-\beta') \quad (45)$$

If we set $\beta' = \beta$ we get

Result 2

$$\sin^2\beta + \sin^2(\beta-\gamma) + \sin^2(\beta+\gamma) = \frac{3}{2} \quad (46)$$

Next consider the expression

$$e^{i\beta} + e^{i(\beta-\gamma)} + e^{i(\beta+\gamma)}$$

we can rearrange this as

$$e^{i\beta}(1 + e^{-i\gamma} + e^{i\gamma}) = e^{i\beta}(1 + 2\cos\gamma)$$

but $\cos\gamma = -\frac{1}{2}$ so that we can write, after taking the real and imaginary parts:

Result 3

$$\sin\beta + \sin(\beta-\gamma) + \sin(\beta+\gamma) = 0.0 \quad (47)$$

Result 4

$$\cos\beta + \cos(\beta-\gamma) + \cos(\beta+\gamma) = 0.0 \quad (48)$$

References

[1] Doisy Y. Port/Starboard Discrimination performances on actived towed arrays systems. *Proceedings of UDT 95*, pp 125-129 (1995).

[2] Van Mierlo G. W. M, Beerens S. P., Been R., Doisy Y. and Trouve E. Port/Starboard Discrimination by hydrophone triplets in active and passive towed arrays. *Proceedings of UDT 97*, pp 176-181 (1997).

[3] Warhonwicz, T., Schmidt-Schierhorn, H. and Hostermann H. Port/Starboard Discrimination Performance by a Twin Line Array for an LFAS sonar system. *Proceedings of UDT Europe 99*, (1999).

[4] Zimmer, W., Private communication.

[5] Smith, S. T., Optimum Phase-Only Adaptive Nulling, *IEEE Transactions On Signal Processing*, **47** (7) pp. 1835-1843 (1999).

[6] Monzingo R A and Miller T W. *Introduction to Adaptive Arrays.* J. Wiley 1980.

[7] Beerens S P, IJsselmuide S P and Volwerk C K, Trouve E and Doisy Y. Flow noise analysis of towed arrays. *Proceedings of UDT 97).*

Document Data Sheet

Security Classification		Project No.
UNCLASSIFIED		04-A
Document Serial No.	**Date of Issue**	**Total Pages**
SR-329	February 2000	44 pp.

Author(s)

Hughes, D.T.

Title

Aspects of cardioid processing

Abstract

It is well known that conventional active towed arrays suffer from 'The Ambiguity Problem' in which it is impossible to distinguish returns from port or starboard. Although operational methods for overcoming this problem exist they are time-consuming and cannot be used for a single ping. One proposed method of coping with these difficulties is to use a triplet array in which the direction of arrival of a signal can be ascertained on a single ping. This report details a broadband algorithm which has been developed and is currently being used at the Saclant Undersea Research Centre. The algorithm was specifically designed to be used on a delay-type beamformer in which shading cannot be applied at the beamlevel. A second algorithm employing the full-flexibility of a 3d beamformer is also described and the two algorithms are compared for their performance in terms of left-right suppression and SNR for which analytical expressions are computed. It is shown that both of the algorithms have desirable but different features. The algorithms are applied to data taken from the trial BACCHUS'98 and the results obtained are used to help validate the theoretical results and to give an indication of the performance which is achievable for the triplet system. We show that for the Centre algorithm a typical achievable left-right suppression is greater than 15dB.

Keywords

Cardioid Processing - left-right suppression - towed array sonar

Issuing Organization

North Atlantic Treaty Organization
SACLANT Undersea Research Centre
Viale San Bartolomeo 400, 19138 La Spezia, Italy

[From N. America: SACLANTCEN (New York) APO AE 09613]

Tel: +39 0187 527 361
Fax:+39 0187 527 700

E-mail: library@saclantc.nato.int

The SACLANT Undersea Research Centre provides the Supreme Allied Commander Atlantic (SACLANT) with scientific and technical assistance under the terms of its NATO charter, which entered into force on 1 February 1963. Without prejudice to this main task - and under the policy direction of SACLANT - the Centre also renders scientific and technical assistance to the individual NATO nations.

This document is approved for public release.
Distribution is unlimited

SACLANT Undersea Research Centre
Viale San Bartolomeo 400
19138 San Bartolomeo (SP), Italy

tel: +39 0187 527 (1) or extension
fax: +39 0187 527 700

e-mail: library@saclantc.nato.int

NORTH ATLANTIC TREATY ORGANIZATION